

International Journal of Modern Physics: Conference Series
 © The Authors

A Novel RF $E \times B$ Spin Manipulator at COSY

Sebastian Mey^{*†} and Ralf Gebel^{*} on behalf of the JEDI Collaboration

^{*} *Institut für Kernphysik, Forschungszentrum Jülich, Wilhelm-Jonen-Str., 52425 Jülich, Germany*

[†] *III. Physikalisches Institut B, RWTH Aachen, Otto-Blumenthal-Str., Aachen, 52074, Germany*

[†] *s.mey@fz-juelich.de*

Received February 18, 2015

The Jülich Electric Dipole Moment Investigations (JEDI) Collaboration is developing tools for the measurement of permanent Electric Dipole Moments (EDMs) of charged, light hadrons in storage rings. While the Standard Model prediction for the EDM gives unobservably small magnitudes, a non-vanishing EDM from \mathcal{CP} violating sources beyond the standard model can lead to a tiny build-up of vertical polarization in a beforehand horizontally polarized beam. This requires a spin tune modulation by an RF dipole without any excitation of coherent beam oscillations. In the course of 2014, a prototype RF $E \times B$ dipole has been successfully commissioned and tested. We verified that the device can be used to continuously flip the vertical polarization of a 970 MeV/c deuteron beam without exciting any coherent beam oscillations.

Keywords: Electric dipole moment; Storage rings; Spin dynamics

PACS numbers:13.40.Em, 11.30.Er, 29.20.db, 29.27.Hj

1. RF Wien-Filter for EDM Experiments

The motion of a relativistic particle's spin in an electromagnetic storage ring ($\vec{\beta} \cdot \vec{B} = \vec{\beta} \cdot \vec{E} = 0$) with non vanishing EDM contributions is given by the generalized *Frenkel-Thomas-BMT* Equation¹, $d\vec{S}/dt = \vec{S} \times \vec{\Omega}$, with

$$\vec{\Omega} = \underbrace{\frac{q}{m} \left((1 + \gamma G) \vec{B} - \left(\gamma G + \frac{\gamma}{\gamma + 1} \right) \vec{\beta} \times \frac{\vec{E}}{c} \right)}_{=:\vec{\Omega}_{\text{MDM}}} + \underbrace{\frac{q}{m} \frac{\eta}{2} \left(\frac{\vec{E}}{c} + \vec{\beta} \times \vec{B} \right)}_{=:\vec{\Omega}_{\text{EDM}}}. \quad (1)$$

Here the anomalous magnetic moment G is given by the particle's Magnetic Dipole Moment (MDM), $\vec{\mu} = 2(G+1) \frac{q\hbar}{2m} \vec{S}$. This corresponds to $G = -0.142$ for deuterons. As an analogue, the dimensionless factor η describes the strength of the particles permanent EDM relative to its MDM. For a Standard Model prediction of $d = \eta \frac{q\hbar}{2mc} \vec{S} \approx 10^{-30}$ e cm its value is $\eta \approx 10^{-15}$.

This is an Open Access article published by World Scientific Publishing Company. It is distributed under the terms of the Creative Commons Attribution 3.0 (CC-BY) License. Further distribution of this work is permitted, provided the original work is properly cited.

In a purely magnetic storage ring, all the terms containing electric fields in Eq. 1 vanish and the EDM contribution due to the interaction with the motional electric field ($\vec{\beta} \times \vec{B}$) will lead to a tiny tilt of the spins precession axis. This leads to a very slow oscillation of the vertical polarization of the circulating beam, but for $\eta \approx 10^{-15}$ its contribution is far below measurable.

A resonant excitation with a radial electric field oscillating on the spin precession frequency would lead to a linear build-up of a vertical component in a horizontally polarized beam, but any RF E field strong enough to yield measurable results would also induce coherent transverse beam oscillations. Therefore a new approach has been proposed.² Instead of using a radial RF E dipole, the accelerator's lattice is supplemented with an RF *Wien*-Filter. According to Eq. 1, the *Lorentz* force cancellation $\vec{E}/c = -\vec{\beta} \times \vec{B}$ means that the device will not influence the EDM directly. It does, however, modulate the horizontal spin precession by means of a phase kick in every turn. Together with the interaction of the EDM with the motional electric field in the rest of the ring, this frequency modulation is able to rotate the spin around the radial axis. The accumulation rate of an EDM signal is then the same as in the *Rabi*-type excitation with an radial electric RF dipole.³

2. Setup of the Prototype

While the above described approach could provide a measurable EDM signal, it doesn't yield a clear observable to characterize the RF *Wien*-Filter itself. Therefore, a first prototype has been commissioned at the **Cooler Synchrotron**⁴ (COSY) in Jülich, Germany, where a radial magnetic field ($\vec{B} = (B_x, 0, 0)^T$) is compensated by a vertical electric field ($\vec{E} = (0, E_y, 0)^T$). In this configuration, the dipole fields directly apply torque onto the vertical component of the particles polarization vector. In the case of *Lorentz* force cancellation, the device is still EDM transparent and expressing the electric field in Eq. 1 in terms of the magnetic field leads to a simple formula for the spin precession in a *Wien*-Filter:³

$$\frac{\vec{E}}{c} = -\vec{\beta} \times \vec{B} \Rightarrow \vec{\Omega}_{\text{wien}} = \frac{q}{m} \left((1 + \gamma G) \vec{B} - \left(\gamma G + \frac{\gamma}{\gamma + 1} \right) \beta^2 \vec{B} \right) = \frac{1 + G}{\gamma} \vec{B}. \quad (2)$$

The particles sample the localized RF fields of the *Wien*-filter once every turn. With the modulation tune defined as the number of RF oscillations per particle revolution, $\nu_m = f_{\text{RF}}/f_{\text{rev}}$, their contribution may be approximated by the integrated field along the particles' path assigned to a point-like device at an orbital angle θ :

$$b(\theta) = \int \hat{B}_x dl \cos(\nu_m \theta + \phi) \sum_{n=-\infty}^{\infty} \delta(\theta - 2\pi n). \quad (3)$$

The resonance strength $|\varepsilon_K|$ of such a device is given by the spin rotation per turn and can be calculated by the *Fourier* integral over one turn in the accelerator:^{5,6}

$$|\varepsilon_K| = \frac{\omega_{\text{spin}}}{\omega_{\text{rev}}} = \frac{1 + G}{2\pi\gamma} \oint \frac{b(\theta)}{B\rho} e^{iK\theta} d\theta = \frac{1 + G}{4\pi\gamma} \frac{\int \hat{B}_x dl}{B\rho} \sum_n e^{\pm i\phi} \delta(n - K \mp \nu_m). \quad (4)$$

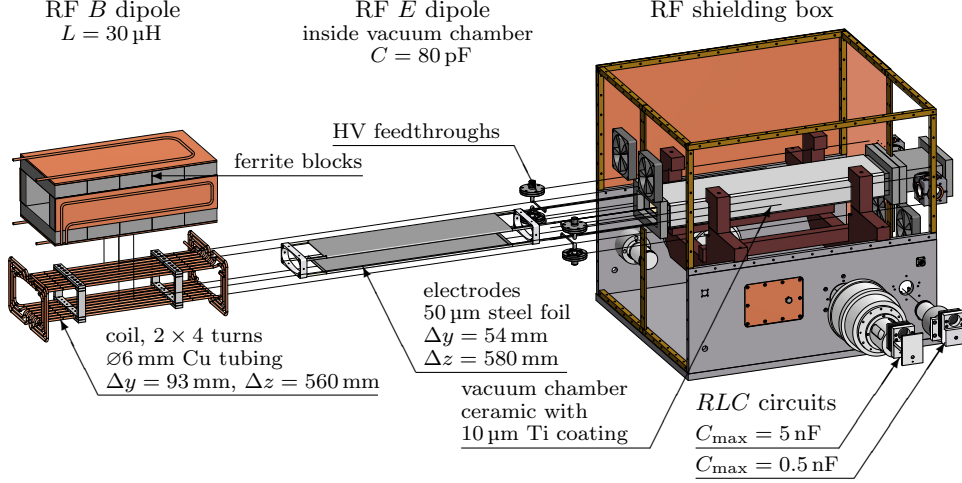


Fig. 1. An explosion drawing showing the main components of the RF $E \times B$ dipole.

An artificial spin resonance occurs at all side-bands with a frequency corresponding to the spin tune:

$$K \stackrel{!}{=} \gamma G = n \pm \nu_m \Leftrightarrow f_{\text{RF}} = f_{\text{rev}} |n - \gamma G|; \quad n \in \mathbb{Z}. \quad (5)$$

In the scope of the current JEDI experiments, deuterons with a momentum of $970 \text{ MeV}/c$ are stored at COSY. In this case, $\gamma = 1.126$ and the resulting spin tune is $\gamma G = -0.1609$. The resulting fundamental mode is located at $f_{\text{RF}} = 121 \text{ kHz}$ with $n = \pm 1$ harmonics at 629 kHz and 871 kHz .

The magnetic RF dipole has been realized in the form of coil wound lengthwise around a ceramic part of the beam-pipe. Water cooling provides stable operating conditions and low-loss, RF capable ferrite blocks improve the homogeneity in the transverse plane. It is driven by means of a parallel resonance circuit with a quality factor of $Q \approx 20$. A similar but separate resonance circuit drives the electric RF dipole. The electric field is generated by the potential difference between two stainless steel electrodes inside the vacuum chamber spanned over glass rods held by a frame inside the flanges of the ceramic beam-chamber. For details see Fig.1.

Without any additional control loops and further dedicated cooling systems it is possible to run the system up to 90 W input power in continuous, long term operation. The maximum current amplitude in the coil is then 5 A leading to an integrated field strength if $\int \hat{B}_x dz = 0.175 \text{ T mm}$. The corresponding integral electric field between the electrodes is $\int \hat{E}_y dz = 24.1 \text{ kV}$.

Fig. 2 shows the distribution of the main component of the *Lorentz* force. Due to different drop-off rates of the electric and magnetic field, particles will get a down-up kick at the entrance and a corresponding up-down kick at the exit of the *Wien-Filter*, but the geometry has been optimized, so that for particles entering the system on axis, the integrated *Lorentz* force along the beam path is set to zero.

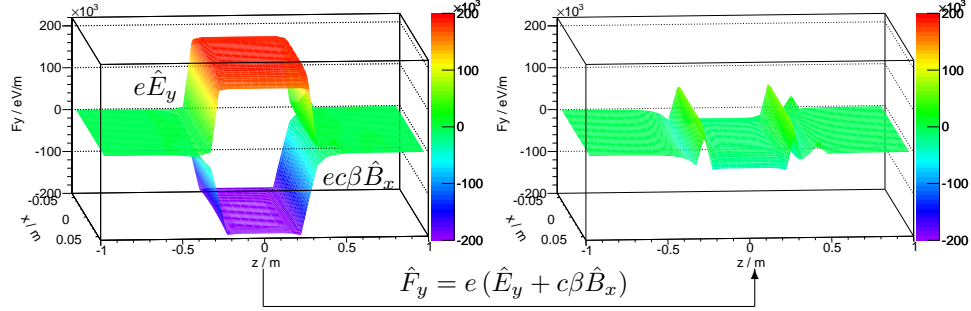
4 *S. Mey & R. Gebel*

Fig. 2. Simulation of the *Lorentz* force plotted across a horizontal cut through the center of the beam pipe ($y = 0$). The results have been normalized to a coil current amplitude of $\hat{I} = 1A$.

3. Measurements

To achieve *Lorentz* force cancellation, the phase as well as the amplitudes of the E and B fields have to be adjusted. The optics of the accelerator was modified so that a vertical betatron sideband was located exactly on top of the frequency of the RF $E \times B$ dipole at 871.52 kHz to achieve maximum sensitivity to induced beam oscillations. Next, the acceptance was limited by installing a massive carbon block directly above the beam as target for the polarimeter. The beam current monitor of COSY could thus be used as a precise tool for the matching of the RF *Wien*-Filter. With a well cooled beam, a sensitivity to amplitude and phase changes in the per mill regime has been achieved. Fig. 3 shows continuous operation of the RF $E \times B$ dipole without inducing additional beam loss.

For polarimetry runs, the deuteron beam is slowly moved onto the carbon target⁷. Polarization manifests itself in the angular distribution of $^{12}\text{C}(\vec{d}, d)$. In case of a vertical polarized beam, this leads to an asymmetry in the event rates of the left (L) and right (R) quadrants of the polarimeter detector. To cancel first-order contributions to systematic errors, the asymmetries were evaluated in terms of the cross ratio CR_Y between of the event rates of the up (\uparrow) and down (\downarrow) polarization states. During the extraction phase, the RF device was operated for 30 s.

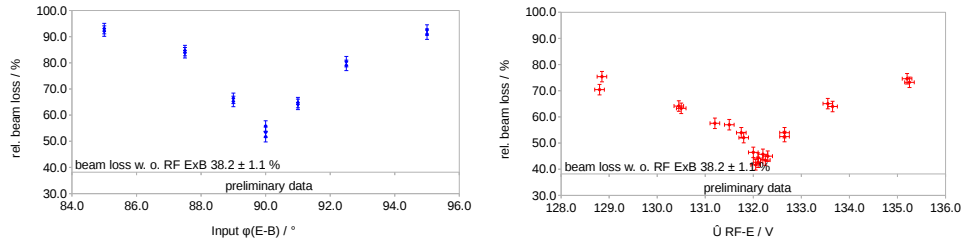


Fig. 3. Measured beam loss while operating the RF $E \times B$ dipole for 30 s. The left panel shows the beam response when varying the input phase as set on the function generators. For the right panel the electrode voltage was varied at a fixed coil current of (232.5 ± 0.6) mA.

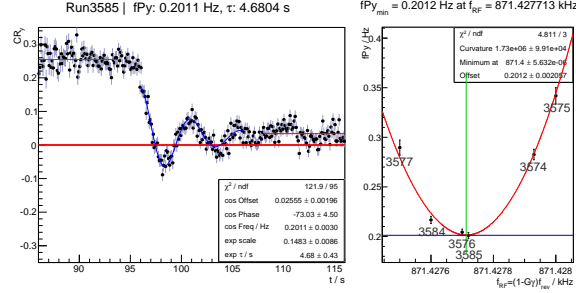


Fig. 4. Example of a fixed frequency scan. The left panel shows the damped, driven oscillation of the vertical polarization component. The oscillation frequency is directly proportional to the resonance strength. The right panel shows fitted frequencies from different runs for varying excitation frequencies. The points form the tip of the spin resonance curve.

Spin-kicks in every turn lead to an adiabatic rotation of the polarization vector, corresponding to an oscillation of its vertical component, in turn represented by the left-right cross-ratio in Fig. 4. The damping of this oscillation is caused by two main sources: the change of momentum during synchrotron oscillations with the associated change in the spin tune γG and the variation of the particles' time of arrival at the RF dipole. A complete spin flip occurs only for an exact match between the exciting RF frequency and the spin resonance frequency, otherwise the excitation will slip beneath the precessing spin. The incomplete spin-flip is then accompanied by an increase in oscillation frequency. This allows the determination of the spin resonance frequency down to ≈ 0.01 Hz with a series of fixed frequency runs scanning the tip of the resonance curve (see left panel of Fig. 4). The frequency of the driven oscillation on resonance is directly proportional to the resonance strength (see Eq. 4).

A series of such fixed frequency scans have been taken during the September 2014 JEDI beam time at COSY to determine the dependence of spin resonance strength upon the betatron tune. Once the *Wien*-Filter was matched at coinciding betatron and spin resonance sidebands, the optics of the accelerator was moved towards different vertical betatron frequencies. For comparison, at each tune a similar scans were taken with an already installed RF solenoid and a pure magnetic RF dipole in form of the new RF $E \times B$ operated without any electric field. Fig. 5 shows this tune dependency. The matched *Wien*-Filter as well as the solenoid don't excite coherent betatron oscillations. As the simple derivation of Eq. 4 suggests, the resonance strength is indeed independent of the vertical betatron tune within the limits of the error bars. In contrast, the simple model doesn't describe the data taken with the magnetic RF dipole at all. The spin motion here is not dominated by the direct spin kick of the RF field, but by the influence of the induced beam oscillations. Experimentally, this effect was already observed by experiments with resonance strength measurements by the SPIN@COSY Collaboration⁸. An analytical solution including the forced betatron motion into the resonance strength can be found in ⁶.

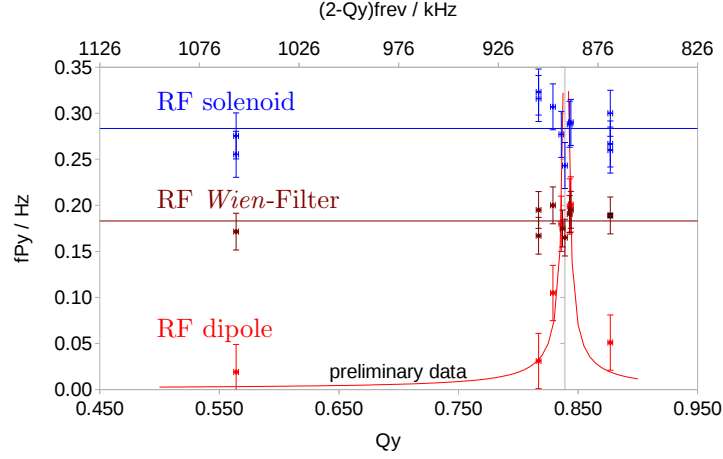
6 *S. Mey & R. Gebel*

Fig. 5. Results of the fixed frequency scans for different fractional vertical betatron tunes. The top scale gives the frequency of the betatron sideband, the vertical line at 871 429.00 Hz is the frequency where the betatron sideband coincides with the spin resonance.

4. Conclusion

As a preparation for future EDM experiments in storage rings, a first prototype of an RF *Wien*-Filter has been commissioned at COSY. We have shown, that this device generates a configuration of RF dipole fields which allow spin manipulation in a storage ring without beam disturbance (see Fig. 5).

Since the cancellation of the *Lorentz* force depends on the particles' velocity spread, beam-based matching of electric and magnetic fields has been tested during the September 2014 JEDI beam-time. Moving the accelerator's betatron sideband so that it coincides with a spin resonance frequency allows a precise determination of the setting for minimum beam disturbance (see Fig. 3).

A slow, stable extraction of particles onto the polarimeter target allows continuous measurement of the beam polarisation for each fill of the COSY accelerator. It is possible to observe the RF field driven oscillation of the vertical polarization component in real time. Determination of the resonance strength then boils down to a frequency measurement (see Fig. 4).

References

1. T. Fukuyama and A. J. Silenko, *Int. J. Mod. Phys. A* **28**, 1350147 (2013).
2. Morse, Orlov and Semertzidis, *Phys. Rev. ST Accel. Beams* **16**, 114001 (2013).
3. K. Nikolaev, http://www.bnl.gov/edm/files/pdf/NNikolaev_Wien_RFE.pdf
4. R. Maier, *NIM A* **390**, 1-8 (1997).
5. M. Bai, W. W. MacKay, and T. Roser, *Phys. Rev. ST Accel. Beams* **8**, 099001 (2005).
6. S. Y. Lee, *Phys. Rev. ST Accel. Beams* **9**, 074001 (2006).
7. Z. Bagdasarian et al., *Phys. Rev. ST Accel. Beams* **17**, 052803 (2014).
8. A. D. Krisch, *Phys. Rev. ST Accel. Beams* **10**, 071001 (2007).